Contents lists available at UGC-CARE

International Journal of Pharmaceutical Sciences and Drug Research

[ISSN: 0975-248X; CODEN (USA): IJPSPP]

Available online at www.ijpsdronline.com

Research Article

Design and Computational Evaluation of New Carbamate Derivatives for the Inhibition of Monoacylglycerol Lipase Enzyme by using Docking

Abhishek Kashyap[1*], Dimpy Rani[1], Suresh Kumar[2], Shailendra Bhatt[1]

[1]*Department of Pharmaceutical Chemistry, School of Medical and Allied Sciences, G. D. Goenka University, Sohna, India.*
[2]*Department of Pharmaceutical Chemistry, Delhi Institute of Pharmaceutical Sciences and Research, Delhi, India.*

ARTICLE INFO

Article history:

Received: 06 August, 2023

Revised: 09 September, 2023

Accepted: 15 September, 2023

Published: 30 September, 2023

Keywords:

Amino acids, Arachidonic Acid, 2-Arachidonoylglycerol, Monoacylglycerol Lipase, Receptors, Enzyme, Endocannabinoid system, Monoacylglycerol lipase inhibitors.

DOI:

10.25004/IJPSDR.2023.150515

ABSTRACT

Different disorders and physiological process have been found to be associated with monoacylglycerol lipase enzyme in humans, like pain, inflammation, and neurodegenerative diseases also. The enzyme is a 33 KDa in weight and a type of serine hydrolase enzyme in nature. The presence of enzyme has been reported in both central and peripheral nervous systems and has show its importance as a key signalling factor in endocannabinoid signalling network system. The enzyme has also reported as source of free fatty acid provider for the cancer cell and tumor growth and their proliferation. In proliferative cancer cells, increased the monoacylglycerol lipase activity is observed. The growth, migration and survival of cancer cells have also found to be associated with phosphatidic acid, lysophosphatidic acid, sphingosine phosphate and prostaglandin E2, which are act as signalling molecules and are found to be derived from free fatty acid. These are also found to be related to the growth, transmission and viability of cancer cells, which increases with the enzyme activity. In the present study we performing computation screening studies of newly designed monoacylglycerol inhibitors which contains carbamate features, these molecules are designed based on previously developed monoacylglycerol carbamate inhibitors.

INTRODUCTION

Monoacylglycerol lipase (MAGL) inhibition is an important target in treatment of cancers and different tumors. It is also found to be beneficial in treatment of psychiatric diseases and some other disorders like retinal disease, inflammation, pain and some nervous system inflammation disorders.[1-3] The hydrolysis of 2-arachidonoylglycerol (2-AG) by MAGL results in the formation of arachidonic acid (AA), a precursor to proinflammatory eicosanoids that promote neuroinflammation and ultimately result in neurodegenerative illnesses including Alzheimer's and Parkinson's disease.[2,4] Inhibitors of MAGL can be effective treatments for many cancers because MAGL is also discovered to be a significant element in the proliferation of several cancer cells.[5-7] The growth and maintenance of the supply of free fatty acids to cancer cells are significantly influenced by MAGL. When compared to nonaggressive tumorigenic cells, aggressive tumor cells frequently exhibit overactivity of MAGL.[8] In the liver and adipose tissues, MAGL participates in the hydrolysis of monoacylglycerol, which supplies a significant amount of free fatty acids (FFAs) for the production of protumorgenic signalling factors as well as the proliferation of cancer cells.[8,9] For both cannabinoid receptors, N-arachidonoylethanolamine (AEA) and 2-arachidinoylglycerol (2-AG) function as ligands and primary endocannabinoids.[10] Endocannabinoids (eCB) are carried to the cytoplasm, where certain enzymes break down these molecules. In contrast to 2-AG, which is primarily hydrolyzed by MAGL by up to 85% into AA[8,11-13] and glycerol, AEA are hydrolyzed by fatty acid amide hydrolase (FAAH) to AA and ethanolamine. Anxiolytic, antiemetic, anti-inflammatory, neuroprotective, and anti-

***Corresponding Author:** Mr. Abhishek Kashyap

Address: Department of Pharmaceutical Chemistry, School of Medical and Allied Sciences, G. D. Goenka University, Sohna, India.

Email ✉**:** abhikash1210@gmail.com

Tel.: +91-9760487370

Relevant conflicts of interest/financial disclosures: The authors declare that the research was conducted in the absence of any commercial or financial relationships that could be construed as a potential conflict of interest.

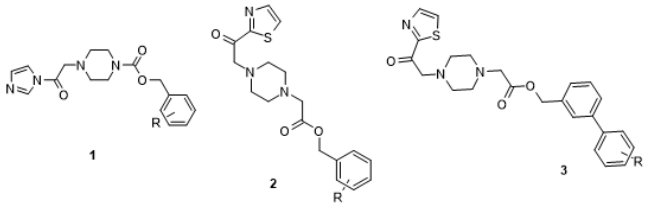

Fig. 1: Images of scaffolds from 1–3 designed on the basis of studies of prior developed carbamate

nociceptive effects can be observed in the brain as a result of the monoacylglycerol lipase being inhibited,[14] which raises the level of 2-AG and activates the neurotransmission system.[15-17] The structure of MAGL consist of an alpha and beta fold and active site, the catalytic triad, which is composed of Ser 122, His 269, and Asp 239, is the name given to the site, which is located in the centre of both the alpha and beta helices.[12,18-22] A large portion of the binding pocket's lipophilic region, which also has amphiphilic and hydrophobic qualities, is known as the acyl carrier binding region (ACB cavity). When 2-AG is attached to the ACB domain (Acyl carrier binding pocket), Ser122 is activated and binds to the carbon that contains the 2-AG carbonyl group.[16] The nucleophilic areas of MAGL also contain binding loops alpha 1 and beta 3, the latter of which contains the residues Ala51, Met123, Gly50, and Gly124. Together, loops alpha 1 and beta 3 are known as oxyanion holes.[23,24] The polarity of these residues interact with a 2-AG hydrophilic portion (Glycerol), which is why the cytoplasmic access channel (CA channel) is another name for the catalytic triad. When the hydrolysis of the catalytic triad is complete, the free fatty acid and glycerol moiety are released.[16] In our current study, we are carrying out computational screening experiments on newly generated monoacylglycerol inhibitors which possess carbamate features. These ligands are designed based on monoacylglycerol carbamate inhibitors that had already been developed. The images of scaffolds is depicted in the Fig. 1. and their corresponding designed derivatives is shown in Tables 1-3.

Materials and Methods

Docking Work Performed

Hardware and software utilised in the study

For the current docking investigations, a 64-bit HP laptop with Windows 11 installed in a single language, an Intel(R) Core TM i3-8130U CPU @ 2.21 GHz, installed 8Gb random access memory (RAM), and a 256 GB SD drive was employed.

Procedure

Using PDB Swiss Viewer, the protein's Apo form was produced in the PDB file, and the ligand was then taken out of the protein-ligand complex and saved as a separate PDB file.[25,26] A library SDF file with 18 proposed variants for each scaffold from 1 to 3 was created using the Open Babel software tool prepared.[27] Three scaffolds made of carbamate analogues were used for designing a total of 54 ligands. The reference ligand and protein were prepared for docking using various wizards, including the Open Babel wizard and the Vina wizard in the PyRx virtual screening tool software, the compound SDF library was converted into PDBQT, and the Apo form of the protein and ligand libraries were docked.[28,29] The ligands were designed and sketched in 2D, SD and other necessarary formats by using ACD/ChemSktech I ACS style and Open Babel GUI tool. For the visualisations of protein and ligand complex, the BIOVIA Discovery studio Visualizer (studio 2020) was utilized. Protein Data Bank (PDB) was a source that was found online to download the crystallographic pdb file.[30,31]

Binding site interactions of ligand with protein

The binding site interaction between the monoacylglycerol lipase enzyme and ligand complex, a catalytic triad, and oxyanion hole residues were all made visible with the aid of BIOVIA Discovery Studio Visualizer 2020. The protein PDB file 5ZUN was used to determine the presence of catalytic triad residues and oxyanion hole residues in the protein-ligand interaction site in order to identify and validate the binding region in the downloaded PDB file of a protein-ligand complex of 5ZUN. The MAGL binding site contains the catalytic triad residues Ser122, His269, and Asp239.[32,33] The residues in the ligand binding site of protein PDB file 5ZUN, which was downloaded from https://www.rcsb.org (Protein data bank), were checked. Ser122, His269, and Asp239 comprise the catalytic triad at the location of the initial ligand-protein contact. Similar to this, oxyanion hole residues Gly50, Ala51, Met123, and Gly124 were observed in the binding site for ligand-protein interactions.[23,24]

Protein Preparation

The monoacylglycerol lipase X-ray crystallographic Structure with the ligand (9JX) with PDB ID: 5ZUN was used for this research. PDB resources were retrieved from https://www.rcsb.org/ (Protein Science - 2017 - Williams – Mol Probity More and Better Reference Data for Improved All-atom Structure Validation. Pdf, n.d.) in the PDB file format for the 3D X-ray crystallographic structure of the protein and ligand, and the MOLPROBITY service was used to prepare the protein's APO form.[34, 35]

In order to fetch the protein from the MOLPROBITY server, the PDB file for the MAGL protein molecule was uploaded as part of the protein preparation process (PDB ID: 5ZUN). Then, we added hydrogens to it and performed the duties of flipping the residues, looking at all the atom connections, and assessing the molecule's geometry using the "Make Flipkin kinemages illustrating any Asn, Gln, or His flips" option. When the software has finished, click "download" to begin downloading the final protein file.

The Apo form of the protein was produced using the Swiss PDB reader and was then prepared for protein production and docking with reference ligands (9JX) and ligands of different designs.

Ligand Preparation

The original ligand 9JX was separated from the protein-ligand combination and saved as a separate file using a Swiss PDB viewer. The docking reference ligand was this file. The three distinct scaffolds used in this investigation were made based on the creation of previously proposed compounds as MAGL inhibitors. The development of the new scaffolds took into account the important traits that were regarded as being similar in the previously developed molecule. From these two scaffolds, 54 different derivatives in all were produced.

Tables 1-3 lists the 54 compounds that were developed for each scaffold and used as ligands. All of the pertinent derivatives' structures were created using the ACD/ ChemSketch molecular structure drawing program, the ACS style option, and the OpenBabel GUI programme. The PyRx virtual screening tool's wizard also makes use of Open Babel when creating ligands in PDBQT format for docking. During the preparation process, all ligands are minimised. Following this, the ligands are converted to the PDBQT format, and the SDF file for the ligand library is entered. The Vina wizard of the PyRx virtual screening programme used the resulting stabilised structures to bind proteins with ligands.

Validation Process

Analysis of the MAGL protein crystal structure's validity using an inhibitor ligand (9JX) (PDB ID: 5ZUN) (4R) -1-(2'-chloro[1,1'-biphenyl]-3-yl) pyrrolidin-2-one, four-[4-(1,3-thiazole-2-carbonyl) piperazin-1-yl]] was finished by redocking the separated ligand file (9JX) from the original PDB file (the ligand's co-crystallized structure) and the Apo form built of the MAGL protein file from 5ZUN into the precise binding site coordinates. For future use, the properties of the grid's coordinates were recorded.

Docking Performed of Prepared Protein and Ligand

The ligands docking procedures were carried out using the Vina wizard in the PyRx virtual screening programme. The produced protein file was downloaded from the MOLPROBITY Server once the Apo protein file was uploaded to it. The downloaded file was then utilised to validate redocking and dock freshly created carbamate derivative ligands from 4 to 54.

The Apo form of the protein and a separate ligand file were created from the protein and ligand complex using the Swiss PDB viewer. The smiles of all the generated ligands were utilised to create the ligand library in SDF format using the Open Babel software. The PyRx virtual screening tool's Open Babel wizard was used to reduce these ligands and convert them to the AutoDock PDBQT format. Next, docking procedures were carried out utilising the AutoDock Vina wizard.[36,37]

For the grid construction process, the grid box's measurements were 25 x 25 x 25 in the x, y, and z directions. The attribute value coordinates were derived from the binding site interactions between the protein and the ligand 9JX from the original PDB file. Each grid point differed from the next by 0.375. The selected grid's X, Y, and Z values are -13.07, 20.8 and -9.6, respectively. With the help of the Auto Dock Vina wizard in the PyRx virtual screening program, each ligand's molecular docking with the generated protein was completed.[38] Using BIOVIA Discovery Studio Visualizer 2020, all docking results for various structures were analysed.[39]

ADME Studies Performed

It is crucial to carry out adsorption, distribution, metabolism, and excretion (ADME) investigations on the molecules in order to further examine the possibility that a created molecule will be used as a significant therapy in the treatment of disease. The SWISSADME web-based tool (http://www.swissadme.ch/), which was used to locate ADME research, was utilised to predict a number of criteria, including lipophilicity (iLOGP, XLOGP3, WLOGP, MLOGP, and SILICOS-IT), solubility in water [Log S (ESOL), Log S (Ali), and Log S (SILICOS-IT)]. Using this SWISSADME web-based application, drug-kinetic characteristics (GI absorption, BBB permeation, P-gp substrate CYP2D6, CYP3A4, CYP1A2, CYP2C19, CYP2C9, inhibitor, Log Kp), medicinal chemistry (PAINS, Brenk, Leadlikeness, Synthetic accessibility), and druglikeness (Bioavailability Score Lipinski, Muegge, Ghose, Veber).[40,41]

The SWISSADME web server was developed and is maintained by the Molecular Modelling Group at the Swiss Institute of Bioinformatics (SIB). Results were obtained by submitting SMILES of different structures and then clicking RUN.

Toxicity Studies Performed

Toxicology studies were performed using the online ADMET prediction tool from the pkCSM web server database, which offers access to the analysis of molecules by drawing or by uploading in SMILES format.[42] AMES toxicity (used to assess the carcinogenic potential of a substance), max. tolerated dose (human), hERG I inhibitor, hERG II inhibitor, oral rat chronic toxicity (LOAEL), oral rat acute toxicity (LD50), skin sensitization, hepatotoxicity, *T. pyriformis* toxicity, and minnow toxicity studies are just a few examples of the toxicity data.

RESULTS

Performed Docking Studies

Target site identification

Two previously created monoacylglycerol lipase inhibitors, JZL184 and Ly218324012, have been reported to function through the catalytic triad of Ser122, Asp239, and His269

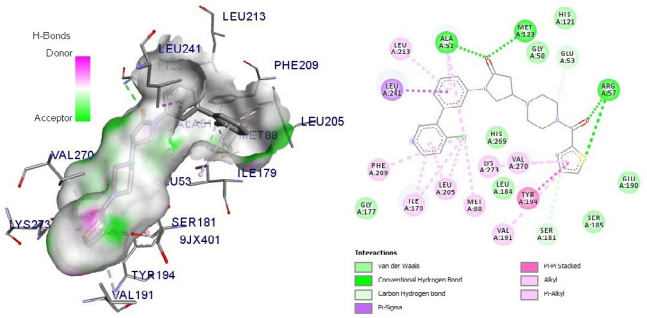

Fig. 2: 3d and 2d images of interactions of original ligand 9JX with residues of MAGL protein 5ZUN.

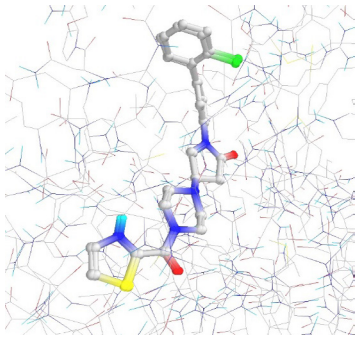

Fig. 3: Image of validation of redocking of ligand 9JX with protein 5ZUN.

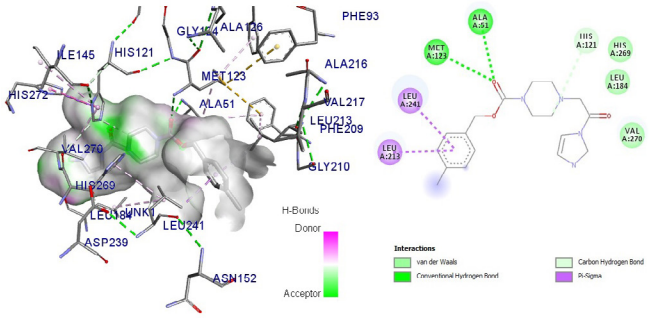

Fig. 4: 3d and 2d images of binding interactions of ligand 8 with residues of 5ZUN

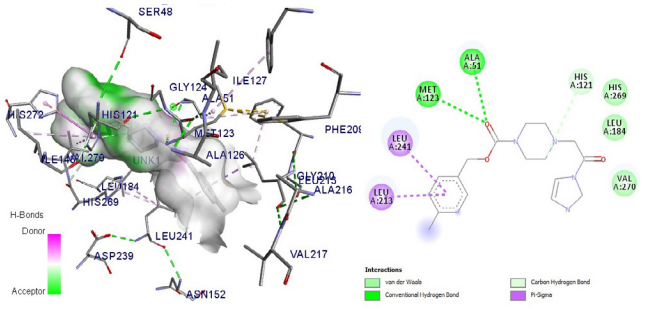

Fig. 5: 3d and 2d images of binding interactions of ligand 20 with residues of 5ZUN

Table 1: Designed 18 ligands from scaffold 1, 4 – 21 and their obtained docking score by docking studies.

S. No.	*Ligand Code*	*Position of R*	*Docking Score*
1.	4	H	-9.4
2	5	4 – NO_2	-9.4
3.	6	3 – NO_2	-9.5
4.	7	2 – NO_2	-9.4
5.	8	4 – Cl	-9.6
6.	9	3 – Cl	-9.4
7.	10	2 – Cl	-9.3
8.	11	4 – F	-9.4
9.	12	3 – F	-9.4
10.	13	2 – F	-9.4
11.	14	4 – Br	-9.4
12.	15	3 – Br	-9.5
13.	16	2 – Br	-9.4
14.	17	4 – OH	-9.1
15.	18	3 – OH	-9.2
16.	19	2 – OH	-9.3
17.	20	4 – CH_3	-9.6
18.	21	3 – CH_3	-9.8

Table 2: Designed 18 ligands from scaffold 2, 22 – 39 and their obtained docking score by docking studies.

S. No.	*Ligand Code*	*Position of R*	*Docking Score*
1.	22	H	-9
2	23	4 – NO_2	-9.2
3.	24	3 – NO_2	-9.2
4.	25	2 – NO_2	-8.7
5.	26	4 – Cl	-8.9
6.	27	3 – Cl	-8.8
7.	28	2 – Cl	-9.2
8.	29	4 – F	-9.4
9.	30	3 – F	-8.6
10.	31	2 – F	-8.8
11.	32	4 – Br	-9.1
12.	33	3 – Br	-8.8
13.	34	2 – Br	-8.8
14.	35	4 – OH	-9.4
15.	36	3 – OH	-8.9
16.	37	2 – OH	-8.8
17.	38	4 – CH_3	-9.1
18.	39	3 – CH_3	-9.4

Table 3: Designed 15 ligands from scaffold 3, 40 – 57 and their obtained docking score by docking studies.

S. No.	*Ligand code*	*Position of R*	*Docking score*
1.	40	H	-10.4
2	41	4 – NO2	-10.6
3.	42	3 – NO2	-10.2
4.	43	2 – NO2	-10.5
5.	44	4 – Cl	-10.3
6.	45	3 – Cl	-11.2
7.	46	2 – Cl	-10.8
8.	47	4 – F	-10.8
9.	48	3 – F	-10.8
10.	49	2 – F	-10.5
11.	50	4 – Br	-10.2
12.	51	3 – Br	-10.4
13.	52	2 – Br	-10.3
14.	53	4 – OH	-10.6
15.	54	3 – OH	-10.6
16.	55	2 – OH	-11
17.	56	4 – CH3	-10.5
18.	57	3 – CH3	-10.8

Table 4: The best top three docking score derivatives from scaffold 1 scaffold 2 and scaffold 3

S. No.	*Scaffold*	*Ligand code*	*Position of R*	*Docking score*
1.	Original Ligand	9JX	-	-13.4
2	Scaffold 1	21	3 – CH_3	-9.8
3.	Scaffold 1	8	4 – Cl	-9.6
4.	Scaffold 1	20	4 – CH_3	-9.6
5.	Scaffold 2	29	4 – F	-9.4
6.	Scaffold 2	35	4 – OH	-9.4
7.	Scaffold 2	39	3 – CH_3	-9.4
8.	Scaffold 3	45	3 – Cl	-11.2
9.	Scaffold 3	55	2 – OH	-11.0
10.	Scaffold 3	46	2 – Cl	-10.8

amino acid residues and form a covalent bond with a serine residue. (Afzal *et al.*, 2016). In the binding area of 9JX, which is depicted in Fig. 2, Ser122, Asp238, and His269 were discovered. The catalytic triad is the ligand's interactions site, according to the MAGL protein-ligand complex 5ZUN PDB file. Similar to this, Gly50, Ala51, Met123, and Gly124

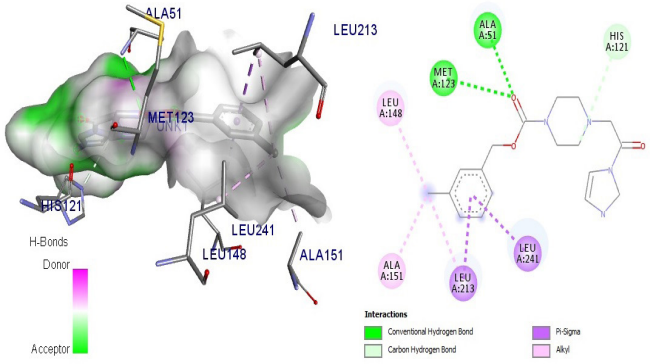

Fig. 6: 3d and 2d images of binding interactions of ligand 21 with residues of 5ZUN

are also present in the docking area of 9JX, indicating the presence of the oxyanion hole, which helps to stabilise the anionic transition state. (Berdan *et al.*, 2016). The same binding region was employed with an expanded grid size of 25 for XYZ dimensions for characteristics X = -13.07, Y = 20.87, and Z = -9.62 in order to cover the full binding zone. These residues in the binding region of 9JX provide proof that the MAGL enzyme has a binding domain.

Validation Studies

The vina wizard in the PyRx programme was used to verify the downloaded MAGL protein with ligand by redocking the ligand (9JX) with a regenerated Apo form of the enzyme MAGL PDB file of 5ZUN. (PDB ID: 5ZUN). It was found that the ideal protein-ligand complex location and the ligand's optimal docking position were both found to be superimposed. The validation studies determined that the binding energy for 9JX was -13.4 kcal/mol. The redocking position is depicted in Figs. 2 and 3. Shows the validation of redocking of ligand 9JX with protein 5ZUN.

Docking Results

The findings of the docking score of the ligands from 4 to 54 with the apo form of the 5ZUN MAGL protein are shown in Tables 1–3. as binding energies with negative values. The top three docking outcomes for each constructed scaffolds from 1–3 are shown in Table 4. ligands altogether, including 18 derivative ligands from each scaffold, scaffold 1, scaffold 2 and scaffold 3, were docked with the apo form of 5ZUN. The best top three docking score derivatives from scaffold 1 scaffold 2 and scaffold 3, were displayed by the ligands 21, 8, 20, from scaffold 1 and their binding interactions is depicted in the Fig. 5-7. Whereas the ligand 29, 35, 39 showed the top three docking score are from scaffold 2, and their binding interactions is depicted in the Fig. 8-10. Similarly 45, 55, 46 are from scaffold 3 and their binding interactions is showed in the Fig. 11-13. The top nine ligands from each scaffold, are listed in Table 5. along with their interactions with residues and hydrogen bonds based on docking scores.

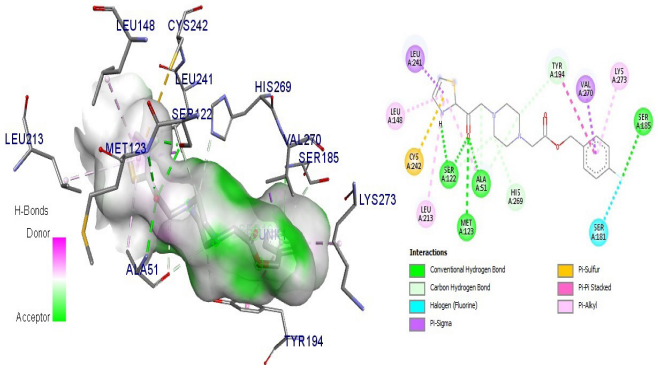

Fig. 7: 3d and 2d images of binding interactions of ligand 29 with residues of 5ZUN

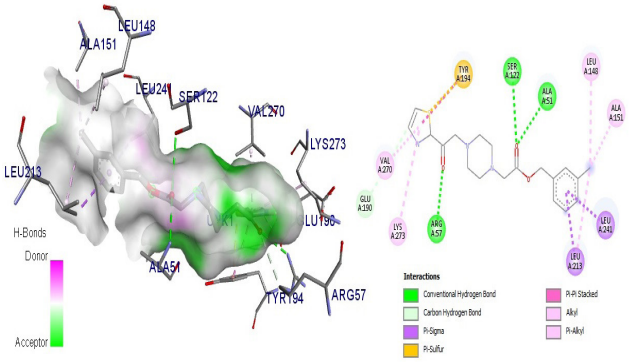

Fig. 9: 3d and 2d images of binding interactions of ligand 39 with residues of 5ZUN

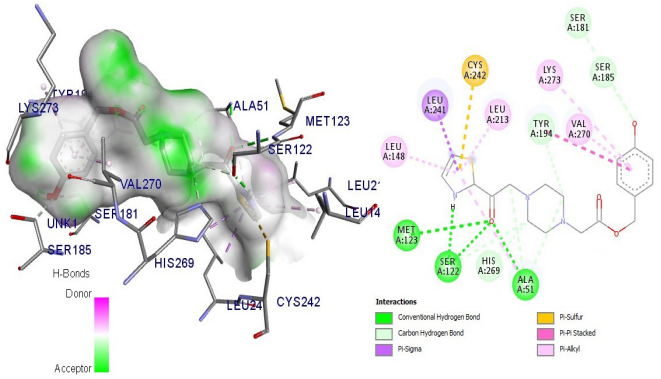

Fig. 8: 3d and 2d images of binding interactions of ligand 35 with residues of 5ZUN

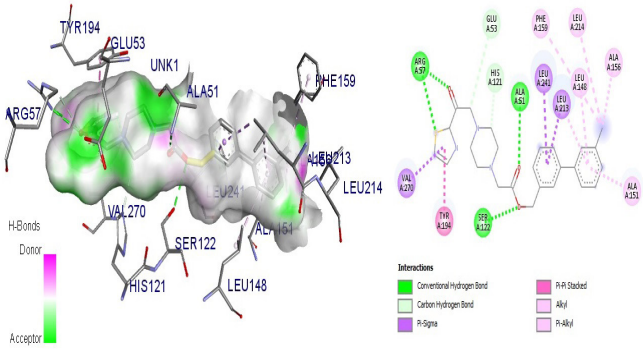

Fig. 10: 3d and 2d images of binding interactions of ligand 45 with residues of 5ZUN

Table 5: Molecular interactions of top scoring ten ligands and reference ligand

S. No.	*Scaffold*	*Ligand code*	*No. of conventional Hydrogen bonds*	*H-bond forming residues*	*H-bond distance (Å)*	*Hydrophobic residues*
1.	Original ligand	Ligand 9JX	3	ALA51, ARG57, MET123	2.09131, 2.14263, 2.19327	LEU241, TYR194, VAL191, VAL270, LYS273, ALA51, ILE179, LEU205
2	Scaffold 1	21	2	ALA51, MET123	2.94111, 3.13805	HIS121, LEU148, LEU213
3.	Scaffold 1	8	2	ALA51, MET123	2.94003, 3.11107	LEU213, LEU241
4.	Scaffold 1	20	2	ALA51, MET123	2.92041, 3.1023	LEU213, LEU241
5.	Scaffold 2	29	5	ALA51, SER122 MET123, SER185, SER122.	2.95862, 3.02058, 3.26397, 3.48701, 2.0624.	LEU241, VAL270, CYS242, TYR194,
6.	Scaffold 2	35	4	ALA51, SER122, MET123, SER122	3.03303, 2.94474, 3.28781, 2.12278	LEU241, CYS242, TYR194
7.	Scaffold 2	39	3	ALA51, ARG57, SER122	2.9262, 2.94596, 3.06044	LEU213, LEU241, ALA151, LEU148, LEU213, VAL270, LYS273
8.	Scaffold 3	45	4	ALA51, ARG57, ARG57 SER122	3.05945 2.9144 3.71945 2.86404 2.53252	LEU213, LEU241, VAL270, ALA156 PHE159
9.	Scaffold 3	55	1	SER122	2.77546	VAL270, VAL270, LYS273, ALA151 ALA156
10.	Scaffold 3	46	2	ALA51, MET123	2.99007 3.12082	LEU213, LEU241, TYR194, ILE179, LEU205

Table 6: ADME studies data of top three molecules of scaffold 1, 2 and scaffold 3

Molecule	*21*	*8*	*20*	*29*	*35*	*39*	*45*	*55*	*46*
MR	100.24	100.19	100.19	103.2	105.26	108.2	133.68	130.7	133.68
TPSA	67.67	67.67	67.67	90.98	111.21	90.98	90.98	111.21	90.98
iLOGP	3.06	3.19	3.1	3.31	2.75	2.95	3.96	3.09	3.46
XLOGP3	1.76	1.5	1.5	2.37	1.91	2.63	4.52	3.54	4.52
WLOGP	1.22	0.87	0.87	1.33	0.48	1.08	3.09	2.15	3.09
MLOGP	1.42	1.15	1.15	0.71	-0.2	0.56	1.91	0.9	1.91
Silicos-IT Log P	1.2	1.07	1.07	3.53	2.63	3.62	5.32	4.2	5.32
Consensus Log P	1.73	1.56	1.54	2.25	1.51	2.17	3.76	2.78	3.66
ESOL Log S	-3.06	-2.77	-2.77	-3.46	-3.16	-3.6	-5.4	-4.67	-5.4
ESOL solubility (mg/mL)	3.15E-01	5.80E-01	5.80E-01	0.131	0.262	0.0944	0.00187	0.00968	0.00187
ESOL solubility (mol/l)	8.67E-04	1.69E-03	1.69E-03	0.000348	0.000698	0.000253	3.98E-06	0.0000214	3.98E-06
ESOL Class	Soluble	Soluble	Soluble	Soluble	Soluble	Soluble	Moderately soluble	Moderately soluble	Moderately soluble
Ali Log S	-2.8	-2.53	-2.53	-3.92	-3.87	-4.19	-6.15	-5.56	-6.15
Ali Solubility (mg/mL)	5.77E-01	1.01E+00	1.01E+00	0.0453	0.0508	0.0241	0.000331	0.00124	0.000331
Ali Solubility (mol/l)	1.59E-03	2.96E-03	2.96E-03	0.00012	0.000135	0.0000644	7.04E-07	2.75E-06	7.04E-07
Ali Class	Soluble	Soluble	Soluble	Soluble	Soluble	Moderately soluble	Poorly soluble	Moderately soluble	Poorly soluble
Silicos-IT LogSw	-3.72	-3.51	-3.51	-4.67	-3.81	-4.78	-7.43	-6.26	-7.43
Silicos-IT Solubility (mg/mL)	6.85E-02	1.06E-01	1.06E-01	0.00816	0.0579	0.00626	0.0000173	0.000248	0.0000173
Silicos-IT Solubility (mol/l)	1.89E-04	3.10E-04	3.10E-04	0.0000216	0.000154	0.0000167	3.69E-08	5.48E-07	3.69E-08
Silicos-IT class	Soluble	Soluble	Soluble	Moderately soluble	Soluble	Moderately soluble	Poorly soluble	Poorly soluble	Poorly soluble
GI absorption	High	High	High	High	High	High	High	High	High
BBB permeant	Yes	No	No	No	No	No	No	No	No
Pgp substrate	No	No	No	No	No	No	No	No	No
log Kp (cm/s)	-7.26	-7.32	-7.32	-6.92	-7.23	-6.71	-5.96	-6.54	-5.96
Lipinski violations	0	0	0	0	0	0	0	0	0
Ghose violations	0	0	0	0	0	0	1	1	1
Veber violations	0	0	0	0	0	0	0	0	0
Egan violations	0	0	0	0	0	0	0	0	0
Muegge violations	0	0	0	0	0	0	0	0	0
Bioavailability score	0.55	0.55	0.55	0.55	0.55	0.55	0.55	0.55	0.55
PAINS alerts	0	0	0	0	0	0	0	0	0
Brenk alerts	0	0	0	0	0	0	0	0	0
Leadlikeness violations	1	0	0	2	2	2	3	3	3
Synthetic accessibility	2.78	2.87	2.91	2.96	2.92	3.07	3.39	3.44	3.44

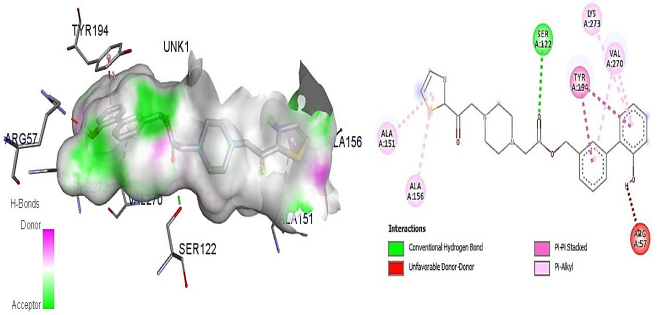

Fig. 11: 3d and 2d images of binding interactions of ligand 55 with residues of 5ZUN

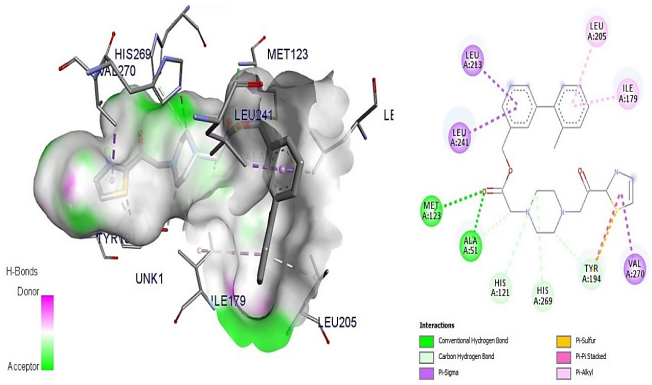

Fig. 12: 3d and 2d images of binding interactions of ligand 46 with residues of 5ZUN

Table 7: Toxicity studies results obtained by using online webserver tool pkCSM for compounds 21, 8, 20, 29, 35, 39, 45, 55 and 46.

Property	*Model name*	*Unit*	*21*	*8*	*20*	*29*	*35*	*39*	*45*	*55*	*46*
Toxicity	AMES toxicity	Categorical (Yes/No)	Yes	Yes	Yes	No	No	No	No	No	No
Toxicity	Max. tolerated dose (human)	Numeric (log mg/kg/day)	0.312	0.327	0.311	0.201	0.033	0.391	0.279	-0.126	0.274
Toxicity	hERG I inhibitor	Categorical (Yes/No)	No	No	No	No	No	No	No	No	No
Toxicity	hERG II inhibitor	Categorical (Yes/No)	Yes	Yes	Yes	Yes	Yes	Yes	Yes	Yes	Yes
Toxicity	Oral rat acute toxicity (LD_{50})	Numeric (mol/kg)	2.83	2.841	2.827	2.577	2.486	2.713	2.587	2.668	2.606
Toxicity	Oral rat chronic toxicity (LOAEL)	Numeric (log mg/kg_bw/day)	0.619	0.67	0.623	1.535	1.496	1.427	2.12	2.081	2.111
Toxicity	Hepatotoxicity	Categorical (Yes/No)	Yes	Yes	Yes	Yes	Yes	Yes	Yes	Yes	Yes
Toxicity	Skin sensitisation	Categorical (Yes/No)	No	No	No	No	No	No	No	No	No
Toxicity	*T. pyriformis* toxicity	Numeric (log ug/L)	0.285	0.285	0.285	0.291	0.289	0.291	0.289	0.287	0.289
Toxicity	Minnow toxicity	Numeric (log mM)	3.793	3.71	3.928	1.207	1.449	0.84	-1.18	-0.655	-1.185

Swiss ADME Studies Results

By utilising the online services of the SwissADME online web server tool, the best nine compounds with the highest docking scores, compounds 21, 8, 20, 29, 35, 39, 45, 55, and 46, were put through the ADME research including (Absorption, Distribution, Metabolism, and Excretion). Better GI absorption was seen in all nine compounds, and none of them violated any of the different drug-likeness parameters. With a strong 0.55 bioavailability rating, Lipinski's five rules include the Ghosh rule, Veber rule, Egan rule, and Muegge rule. Each of the nine compounds also shown good synthetic accessibility. Calculations were also made for additional criteria such LogP, molar refractivity, TPSA value, XLOGP3, WLOGP, and MLOGP. The outcomes are shown in Table 6.

Toxicity Studies Results

The pkCSM server online tool was used to perform toxicity prediction studies for all the molecules according to their docking score. All the nine best docking score molecules were found safe hERG I inhibitor (cardiotoxicity) and found toxic for hERG II. All the compounds also showed toxicity towards hepatotoxicity profile. The results of toxicities studies are given in Table 7.

Discussion

Based on analyses of previously established compounds and their key characteristics for activity, this study was carried out to find the newly designed and developed new scaffolds. We created 54 ligands by altering the features, and in this study, these were assessed using docking as well as other online web servers for pharmacokinetic ADME prediction, such as SwissADME and pkCSM tool, in order to find more effective and secure moiety for the treatment of cancer and other neuroinflammatory diseases as well as for other target diseases as MAGL inhibitors. The top nine docking scores, or the three best compounds from each scaffold 1, 2, and 3, which are 22, 8, 20, 29, 35, 39, 45, and

55 and 46, were used to determine the top powerful agents. These top nine scoring ligands were further assessed for toxicity studies using the pkCSM online tool and ADME prediction studies using the SwissADME online web server tool. All the nine compounds demonstrated improved GI absorption, high synthetic accessibility, and no violations of any of the drug-likeness criteria.

Acknowledgments

Here we would like to thanks PyRx sourceforge, Swiss Institute of Bioinformatics (SwissADME online server tool) and pkCSM online webserver tool providers for using there tools.

Reference

1. Ahamed M, Attili B, van Veghel D, Ooms M, Berben P, Celen S, Koole M, Declercq L, Savinainen JR, Laitinen JT, Verbruggen A, Bormans G. Synthesis and preclinical evaluation of [11C]MA-PB-1 for in vivo imaging of brain monoacylglycerol lipase (MAGL). Eur J Med Chem. 2017; 136:104–13.
2. Kokona D, Spyridakos D, Tzatzarakis M, Papadogkonaki S, Filidou E, Arvanitidis KI, Kolios G, Lamani M, Makriyannis A, Malamas MS, Thermos K. The endocannabinoid 2-arachidonoylglycerol and dual ABHD6/MAGL enzyme inhibitors display neuroprotective and anti-inflammatory actions in the in vivo retinal model of AMPA excitotoxicity. Neuropharmacology. 2021; 185:108450.
3. Zhu B, Connolly PJ, Zhang YM, McDonnell ME, Bian H, Lin SC, Liu L, Zhang SP, Chevalier KM, Brandt MR, Milligan CM, Flores CM, Macielag MJ. The discovery of azetidine-piperazine di-amides as potent, selective and reversible monoacylglycerol lipase (MAGL) inhibitors. Bioorganic Med Chem Lett. 2020; 30:127243.
4. Korhonen J, Kuusisto A, Van Bruchem J, Patel JZ, Laitinen T, Navia-Paldanius D, Laitinen JT, Savinainen JR, Parkkari T, Nevalainen TJ. Piperazine and piperidine carboxamides and carbamates as inhibitors of fatty acid amide hydrolase (FAAH) and monoacylglycerol lipase (MAGL). Bioorganic Med Chem. 2014; 22:6694–6705.
5. Zhu B, Connolly PJ, Zhang SP, Chevalier KM, Milligan CM, Flores CM, Macielag MJ. The discovery of diazetidinyl diamides as potent and reversible inhibitors of monoacylglycerol lipase (MAGL). Bioorganic Med Chem Lett. 2020; 30:127198.
6. Grimsey NL, Savinainen JR, Attili B, Ahamed M. Regulating membrane lipid levels at the synapse by small-molecule inhibitors of monoacylglycerol lipase: new developments in therapeutic and PET imaging applications. Drug Discov Today. 2020; 25:330–43.
7. Gruden E, Kienzl M, Hasenoehrl C, Sarsembayeva A, Ristic D, Theresa S, Maitz K, Taschler U, Hahnefeld L, Gurke R, Thomas D, Kargl J, Schicho R. Prostaglandins , Leukotrienes and Essential Fatty Acids Tumor microenvironment-derived monoacylglycerol lipase provokes tumor-specific immune responses and lipid profiles. Prostaglandins, Leukot Essent Fat Acids. 2023; 196:102585.
8. Poli G, Lapillo M, Jha V, Mouawad N, Caligiuri I, Macchia M, Minutolo F, Rizzolio F, Tuccinardi T, Granchi C. Computationally driven discovery of phenyl(piperazin-1-yl)methanone derivatives as reversible monoacylglycerol lipase (MAGL) inhibitors. J Enzyme Inhib Med Chem. 2019. doi:10.1080/14756366.2019.1571271.
9. Tuccinardi T, Granchi C, Rizzolio F, Caligiuri I, Battistello V, Toffoli G, Minutolo F, Macchia M, Martinelli A. Identification and characterization of a new reversible MAGL inhibitor. Bioorganic Med Chem. 2014; 22:3285–91.
10. He Y, Gobbi LC, Herde AM, Rombach D, Ritter M, Kuhn B, Wittwer MB, Heer D, Hornsperger B, Bell C, O'Hara F, Benz J, Honer M, Keller C, Collin L, Richter H, Schibli R, Grether U, Mu L. Discovery, synthesis and evaluation of novel reversible monoacylglycerol lipase radioligands bearing a morpholine-3-one scaffold. Nucl Med Biol. 2022; 108–109:24–32.
11. Ahamed M, Attili B, van Veghel D, Ooms M, Berben P, Celen S, Koole M, Declercq L, Savinainen JR, Laitinen JT, Verbruggen A, Bormans G. Synthesis and preclinical evaluation of [11C]MA-PB-1 for in vivo imaging of brain monoacylglycerol lipase (MAGL). Eur J Med Chem. 2017. doi:10.1016/j.ejmech.2017.04.066.
12. Chen Z, Mori W, Fu H, Schafroth MA, Hatori A, Shao T, Zhang G, Van RS, Zhang Y, Hu K, Fujinaga M, Wang L, Belov V, Ogasawara D, Giffenig P, Deng X, Rong J, Yu Q, Zhang X, Papisov MI, Shao Y, Collier TL, Ma JA, Cravatt BF, Josephson L, Zhang MR, Liang SH. Design, Synthesis, and Evaluation of 18F-Labeled Monoacylglycerol Lipase Inhibitors as Novel Positron Emission Tomography Probes. J Med Chem. 2019. doi:10.1021/acs.jmedchem.9b00936.
13. Bononi G, Tonarini G, Poli G, Barravecchia I, Caligiuri I, Macchia M, Rizzolio F, Demontis GC, Minutolo F, Granchi C, Tuccinardi T. Monoacylglycerol lipase (MAGL) inhibitors based on a diphenylsulfide-benzoylpiperidine scaffold. Eur J Med Chem. 2021; 223:113679.
14. Xu J, Zheng G, Hu J, Ge W, Bradley JL, Ornato JP, Tang W. The monoacylglycerol lipase inhibitor, JZL184, has comparable effects to therapeutic hypothermia, attenuating global cerebral injury in a rat model of cardiac arrest. Biomed Pharmacother. 2022; 156:113847.
15. Zhang L, Butler CR, Maresca KP, Takano A, Nag S, Jia Z, Arakawa R, Piro JR, Samad T, Smith DL, Nason DM, O'Neil S, McAllister L, Schildknegt K, Trapa P, McCarthy TJ, Villalobos A, Halldin C. Identification and Development of an Irreversible Monoacylglycerol Lipase (MAGL) Positron Emission Tomography (PET) Radioligand with High Specificity. J Med Chem. 2019. doi:10.1021/acs.jmedchem.9b00847.
16. Mori W, Hatori A, Zhang Y, Kurihara Y, Yamasaki T, Xie L, Kumata K, Hu K, Fujinaga M, Zhang MR. Radiosynthesis and evaluation of a novel monoacylglycerol lipase radiotracer: 1,1,1,3,3,3-hexafluoropropan-2-yl-3-(1-benzyl-1H-pyrazol-3-yl)azetidine-1-[11C]carboxylate. Bioorganic Med Chem. 2019; 27:3568–73.
17. Aghazadeh Tabrizi M, Baraldi PG, Baraldi S, Ruggiero E, De Stefano L, Rizzolio F, Di Cesare Mannelli L, Ghelardini C, Chicca A, Lapillo M, Gertsch J, Manera C, Macchia M, Martinelli A, Granchi C, Minutolo F, Tuccinardi T. Discovery of 1,5-Diphenylpyrazole-3-Carboxamide Derivatives as Potent, Reversible, and Selective Monoacylglycerol Lipase (MAGL) Inhibitors. J Med Chem. 2018; 61:1340–54.
18. Cheng B, Yuan WE, Su J, Liu Y, Chen J. Recent advances in small molecule based cancer immunotherapy. Eur. J. Med. Chem. 2018. doi:10.1016/j.ejmech.2018.08.028.
19. Afzal O, Akhtar MS, Kumar S, Ali MR, Jaggi M, Bawa S. Hit to lead optimization of a series of N-[4-(1,3-benzothiazol-2-yl) phenyl]acetamides as monoacylglycerol lipase inhibitors with potential anticancer activity. Eur J Med Chem. 2016. doi:10.1016/j.ejmech.2016.05.038.
20. Scalvini L, Vacondio F, Bassi M, Pala D, Lodola A, Rivara S, Jung KM, Piomelli D, Mor M. Free-energy studies reveal a possible mechanism for oxidation-dependent inhibition of MGL. Sci Rep. 2016; 6:1–12.
21. Ma M, Bai J, Ling Y, Chang W, Xie G, Li R, Wang G, Tao K. Monoacylglycerol lipase inhibitor JZL184 regulates apoptosis and migration of colorectal cancer cells. Mol Med Rep. 2016; 13:2850–56.
22. Lauria S, Casati S, Ciuffreda P. Synthesis and characterization of a new fluorogenic substrate for monoacylglycerol lipase and application to inhibition studies. Anal Bioanal Chem. 2015; 407:1–5.
23. Berdan CA, Erion KA, Burritt NE, Corkey BE, Deeney JT. Inhibition of monoacylglycerol lipase activity decreases glucose-stimulated insulin secretion in INS-1 (832/13) cells and rat islets. PLoS One. 2016; 11:e0149008.
24. Sherer C, Snape TJ. Heterocyclic scaffolds as promising anticancer agents against tumours of the central nervous system: Exploring the scope of indole and carbazole derivatives. Eur. J. Med. Chem. 2015; 97:552–60.
25. Swain C. Open Babel Documentation. 2014.
26. Doganc F, Celik I, Eren G, Kaiser M, Brun R, Goker H. Synthesis, in vitro antiprotozoal activity, molecular docking and molecular dynamics studies of some new monocationic guanidinobenzimidazoles. Eur J Med Chem. 2021; 221:113545.

27. O'Boyle NM, Banck M, James CA, Morley C, Vandermeersch T, Hutchison GR. Open Babel. J Cheminform. 2011; 3:1–14.
28. Dain FA, Opo M, Rahman MM, Ahammad F, Ahmed I, Bhuiyan A, Asiri AM. Structure based pharmacophore modeling, virtual screening, molecular docking and ADMET approaches for identification of natural anti-cancer agents targeting XIAP protein. Sci Reports |. 123AD; 11:4049.
29. Tannas LE. System Requirements. Flat-Panel Displays CRTs. 1985;:31–53.
30. Berman HM, Westbrook J, Feng Z, Gilliland G, Bhat TN, Weissig H, Shindyalov IN, Bourne PE. The Protein Data Bank. Nucleic Acids Res. 2000; 28:235–42.
31. Protein Science - 2017 - Williams - MolProbity More and better reference data for improved all-atom structure validation.pdf. .
32. Bononi G, Granchi C, Lapillo M, Giannotti M, Nieri D, Fortunato S, Boustani M El, Caligiuri I, Poli G, Carlson KE, Kim SH, Macchia M, Martinelli A, Rizzolio F, Chicca A, Katzenellenbogen JA, Minutolo F, Tuccinardi T. Discovery of long-chain salicylketoxime derivatives as monoacylglycerol lipase (MAGL) inhibitors. Eur J Med Chem. 2018; 157:817–36.
33. Riccardi L, Arencibia JM, Bono L, Armirotti A, Girotto S, De Vivo M. Lid domain plasticity and lipid flexibility modulate enzyme specificity in human monoacylglycerol lipase. Biochim Biophys Acta - Mol Cell Biol Lipids. 2017; 1862:441–51.
34. Chen VB, Arendall WB, Headd JJ, Keedy DA, Immormino RM, Kapral GJ, Murray LW, Richardson JS, Richardson DC. MolProbity : all-atom structure validation for macromolecular crystallography . 2012;:694–701.
35. Davis IW, Leaver-Fay A, Chen VB, Block JN, Kapral GJ, Wang X, Murray LW, Arendall WB, Snoeyink J, Richardson JS, Richardson DC. MolProbity: all-atom contacts and structure validation for proteins and nucleic acids. Nucleic Acids Res. 2007; 35:W375–83.
36. Eberhardt J, Santos-Martins D, Tillack AF, Forli S. AutoDock Vina 1.2.0: New Docking Methods, Expanded Force Field, and Python Bindings. J Chem Inf Model. 2021; 61:3891–98.
37. Allouche A. Software News and Updates Gabedit — A Graphical User Interface for Computational Chemistry Softwares. J Comput Chem. 2012; 32:174–82.
38. Carolina A, De Sousa C, Combrinck JM, Maepa K, Egan TJ. Virtual screening as a tool to discover new β-haematin inhibitors with activity against malaria parasites. doi:10.1038/s41598-020-60221-0.
39. Studio 2020 BD. Dassault Systems: San Diego. CA, USA. 2020.
40. Pires DEV, Blundell TL, Ascher DB. pkCSM: Predicting small-molecule pharmacokinetic and toxicity properties using graph-based signatures. J Med Chem. 2015; 58:4066–72.
41. Daina A, Michielin O, Zoete V. SwissADME: A free web tool to evaluate pharmacokinetics, drug-likeness and medicinal chemistry friendliness of small molecules. Sci Rep. 2017; 7:1–13.
42. Afzal O, Kumar S, Kumar R, Firoz A, Jaggi M, Bawa S. Docking based virtual screening and molecular dynamics study to identify potential monoacylglycerol lipase inhibitors. Bioorganic Med Chem Lett. 2014; 24:3986–96.

HOW TO CITE THIS ARTICLE: Kashyap A, Rani D, Kumar S, Bhatt S. Design and Computational Evaluation of New Carbamate Derivatives for the Inhibition of Monoacylglycerol Lipase Enzyme by using Docking. Int. J. Pharm. Sci. Drug Res. 2023;15(5):665-674. **DOI:** 10.25004/IJPSDR.2023.150515